



The promise of cryo-EM to explore RNA structural dynamics

Steve L. Bonilla¹ and Jeffrey S. Kieft^{1,2*}

1 - Department of Biochemistry and Molecular Genetics, Aurora, CO 80045, USA

2 - RNA BioScience Initiative, University of Colorado Anschutz Medical Campus, School of Medicine, Aurora, CO 80045, USA

Correspondence to Jeffrey S. Kieft:*Department of Biochemistry and Molecular Genetics, University of Colorado School of Medicine, Mail Stop 8101, Aurora, CO 80045, USA. Jeffrey.Kieft@cuanschutz.edu (J.S. Kieft)

@Steve_Bonilla (S.L. Bonilla), @JeffreyKieft (J.S. Kieft)

<https://doi.org/10.1016/j.jmb.2022.167802>

Edited by Philip C. Bevilacqua

Abstract

Conformational dynamics are essential to macromolecular function. This is certainly true of RNA, whose ability to undergo programmed conformational dynamics is essential to create and regulate complex biological processes. However, methods to easily and simultaneously interrogate both the structure and conformational dynamics of fully functional RNAs in isolation and in complex with proteins have not historically been available. Due to its ability to image and classify single particles, cryogenic electron microscopy (cryo-EM) has the potential to address this gap and may be particularly amenable to exploring structural dynamics within the three-dimensional folds of biologically active RNAs. We discuss the possibilities and current limitations of applying cryo-EM to simultaneously study RNA structure and conformational dynamics, and present one example that illustrates this (as of yet) not fully realized potential.

© 2022 The Authors. Published by Elsevier Ltd. This is an open access article under the CC BY-NC-ND license (<http://creativecommons.org/licenses/by-nc-nd/4.0/>).

Introduction

RNAs form intricate, conformationally dynamic secondary and tertiary (3°) structures that are essential for regulating diverse biological processes, thus a critical goal for biomedical research is to solve these structures and understand how they determine biological function.^{1–3} However, the study of RNA structure–function relationships is challenged by the dynamic nature of RNA structure. Although cryogenic electron microscopy (cryo-EM) is rapidly emerging as a premier structural biology tool, its use to infer functional conformational dynamics of structured RNAs, both free and/or bound to protein partners, has not been fully exploited. Here, we will discuss the dynamic nature of RNA structure and the associated experimental challenges, present examples of how cryo-EM can help address some of these

challenges, and discuss the promise and limitations of the method as a tool to study RNA conformational dynamics.

RNA structures comprise dynamic conformational ensembles

In solution, every macromolecule fluctuates between a large number of conformational states, collectively referred to as its ‘conformational ensemble’ (Figure 1).^{4–5} Dependent on intrinsic molecular properties and environmental conditions, some states of the ensemble are more prevalent (i.e., more stable) than others, but even rare states can be important for function. Although all macromolecules are conformationally dynamic, in practice a distinction is made between ‘rigid’ and ‘flexible’ molecules. These qualitative terms can have different contextual meanings, but typically a molecule is

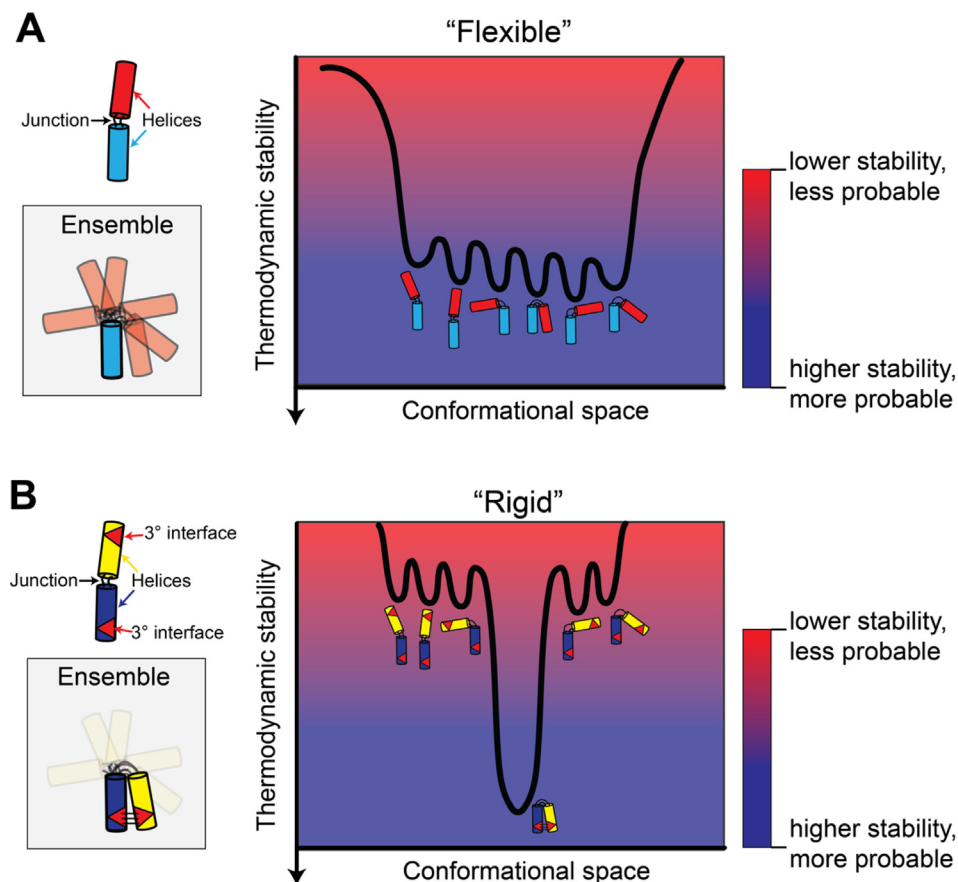


Figure 1. Schematics comparing the energy landscape of macromolecules with “flexible” and “rigid” conformational ensembles. Helices are represented as cylinders and junctions as connecting strings. **(A)** Energy landscape shows multiple conformational states (i.e., energy wells) with similar thermodynamic stabilities. Because the states have similar stabilities and there are relatively low energy barriers between them, they are approximately equally occupied at any time (i.e., they have equal probabilities). The ensemble illustrated in the left box shows superposition of possible conformational states, each of them equally represented in the ensemble, illustrated using transparency levels. Molecules displaying this type of conformational behavior are typically referred to as “flexible”. **(B)** Energy landscape shows one conformation that is much more stable than the rest of the conformations in the ensemble. In this hypothetical case, additional stability is contributed by the formation of long-range contacts between 3° interfaces (red triangles). The conformation with high stability is much more probable and occupied than the rest of the conformations. The ensemble on the left box illustrates this point by making the stable conformation opaquer than the rarer (transparent) conformations. Molecules displaying this type of conformational behavior are typically referred to as “rigid”.

referred to as ‘flexible’ when, under the experimental conditions, it fluctuates between a relatively large number of similarly stable conformational states (Figure 1(A)). In contrast, ‘rigid’ molecules populate one or a limited number of well-defined states, while other states of the ensemble are much less stable and therefore rarely populated (Figure 1(B)). Using these terms for convenience, folded RNAs tend to be significantly more flexible than folded proteins, due to intrinsic differences in the architectures of these macromolecules. Many complex RNA 3° structures are collections of short, modular helices connected by relatively flexible junctions serving as “hinges” that orient helices in different directions relative to each other.¹ The helices are stabilized

locally by base stacking and base pairing and may interact with distant helices only at limited 3° contact interfaces. Thus, in contrast to the densely packed structures of proteins that are stabilized by extensive networks of long-range contacts and the hydrophobic effect, many RNAs are more loosely packed and stabilized by a relatively small set of sparsely distributed 3° contacts, resulting in a greater degree of local structural fluctuations and inter-domain movements.^{1,6} Additionally, due to the promiscuity of base–base interactions, a single RNA sequence can specify very different but similarly stable secondary and 3° structures, further increasing the potential structural complexity of the ensemble.¹ As described below, flexible and/

or conformationally heterogeneous molecules tend to be very challenging targets for structural biology and, therefore, there is a plethora of functional RNAs with unknown three-dimensional (3D) structures. Solving the major conformations adopted by these RNAs and dissecting their structural dynamics are essential steps towards a mechanistic understanding of RNA function. Additionally, because distinct RNA 3° structures typically consist of sets of recurring motifs – i.e., RNA structure is modular – lessons learned from dissecting the conformational ensembles of specific RNAs can often inform on principles applicable across diverse RNA sequences.^{7–11}

The importance of conformational dynamics to RNA function

To function, RNAs interact with many different proteins, ions, small molecules, and/or other RNAs, and conformational dynamics frequently play a role in these interactions.^{4,12–13} Often, the interaction partners recognize one or more specific states within the conformational ensemble of the RNA, but not all states. This ‘conformational selection’ mechanism, in which the RNA samples the bound conformation prior to ligand binding, depends on the dynamic sampling of multiple states, and evidence suggests that it is a major mode of RNA molecular recognition.⁴ For example, riboswitches are structured elements, mostly found in the 5′ untranslated regions (UTRs) of bacterial mRNAs, that turn gene expression ‘on’ or ‘off’ (i.e., a two-state switch) in a ligand-dependent manner by adopting mutually exclusive ligand-free and ligand-bound conformational states.¹⁴ Nuclear magnetic resonance (NMR) and fluorescence microscopy studies showed that, in the absence of ligand, the S-adenosylmethionine type II (SAM-II) riboswitch explores multiple conformational states and transiently adopts a conformation that resembles the ligand-bound state, which is “captured” and stabilized by ligand binding.¹⁵ Other riboswitches use similar conformationally dynamic mechanisms.¹³ The ensemble nature of RNA can also be important during the assembly of large RNA-protein complexes. For example, during ribosome assembly, the binding of proteins can select specific rRNA conformational states, steering the assembly pathway to reach the correct final structure.¹⁶ In addition to conformational selection, another mode of RNA molecular recognition is induced fit, in which conformational changes occur after binding of the ligand; the ligand dissociation rate is slower than formation of the induced conformation.¹⁷ In practice it can be difficult to distinguish between conformational selection and induced fit, but both are important mechanisms that involve RNA conformational dynamics. For more examples of canonical RNA dynamics-function relationships see ref.⁴ Recently, it has become clear that genomes are extensively transcribed and produce

thousands of long non-coding RNAs (lncRNAs).^{18–19} Although the functions of most lncRNAs are unknown (and debated), many of them likely depend on molecular recognition and therefore on structure and conformational dynamics.

The challenge of studying conformationally dynamic RNA structures

Despite the central role of structural dynamics in creating and regulating function, experimentally visualizing the full conformational ensemble of an RNA is impossible because all techniques have limited spatial and temporal resolutions. However, in many cases structural characterization of a small subset of states can provide a useful approximation of the ensemble and/or can be combined with computational modelling to infer conformations that are not accessible experimentally.^{10,20–22} Multiple states may be detected simultaneously, i.e., in a single experiment, or be captured biochemically, pharmacologically, or genetically and examined individually. In some cases, structural dynamics can be inferred from experimental uncertainty or “fuzziness”, analogous to a blurry photograph of a moving object. Therefore, although these methods do not provide a comprehensive picture of the ensemble, they can generate testable hypotheses, guide biophysical studies, and eventually lead to a mechanistic understanding of structure-dynamics-function relationships.

X-ray crystallography has greatly contributed to our understanding of RNA structure. Although this technique does not directly report on structural dynamics, in some cases a single crystal can contain multiple conformations, ‘snapshots’ of different states can be captured and crystallized individually, and/or relatively disordered parts of the molecule in the crystallized state can suggest local flexibility.^{23–24} However, the crystallization requirement tends to favor overall rigid molecules and/or bias the sample into adopting particular conformational states.^{25–26}

NMR can query the molecules in solution and can access conformational dynamics within a wide range of timescales.^{21,27} With the help of computational modelling, NMR yields experimentally supported conformational ensembles of small RNAs and can reveal conformational rearrangements within larger functional RNAs.²² However, this technique is mostly reserved for relatively small RNAs (<100 nts) or smaller regions or interactions within larger RNAs, and is limited by the time-consuming and labor-intensive challenge of assigning the resonances.²⁸

Other powerful methods for probing RNA structural dynamics include single-molecule Förster resonance energy transfer (smFRET), X-ray scattering, chemical probing, and high-throughput binding measurements.^{9–11,29–33} In particular, although a low-resolution technique, small

angle X-ray scattering (SAXS) has been an invaluable tool for probing RNA folding and conformational changes in solution.^{30,34–38} Each of these methods have specific strengths and limitations in the type, number, timescale, and stability of the conformations that can be detected, and often a combination of techniques needs to be applied for a mechanistic understanding of RNA structure-dynamics-function relationships. Ultimately, how many conformations within the full ensemble need to be probed and the best methods to probe those conformations depend on the RNA and the biological question of interest.

Advances in the determination of protein-free RNA structures by cryo-EM

Recent advances in instrumentation and data processing tools have led to a “resolution revolution” in single particle cryo-EM.^{39–41} Typical targets of cryo-EM are large assemblies of proteins and nucleic acids (e.g., the ribosome) but the advances that caused the resolution revolution have also had the effect that smaller and more flexible structures can be solved.⁴² These advances have mostly benefited the protein structure field and the study of large RNA-protein complexes like the ribosome, but recent studies have demonstrated their applicability to protein-free functional RNAs.²⁶ To date, cryo-EM has been used to solve RNAs as small as a 40 kDa riboswitch to 3.7 Å resolution and provided three structures with <3.5 Å resolution.^{43–45} The technique has also been applied to challenging RNA targets, such as conformationally dynamic viral RNAs and kinetically trapped RNA folding intermediates.^{46–48} These advances in RNA-only cryo-EM have been made possible not only by advances in microscopes and detectors, but also by the development of computational tools for fitting atomic models of RNA into low- to moderate-resolution maps and by the engineering of RNA constructs with modular structural modifications, such as localized helical extensions, that provide modelling constraints.^{45–46,49} As a recently published review article describes advances in the use of single-particle cryo-EM for structural determination of protein-free RNAs,²⁶ we focus the rest of our discussion on the use of cryo-EM and computational tools for inferring RNA structural dynamics.

Opportunities and challenges of cryo-EM for the study of RNA structural dynamics

One of the main advantages of cryo-EM over X-ray crystallography is that the sample does not require crystallization and therefore does not bias the particles into a particular conformational state. Instead, the sample is prepared by rapidly cooling the particles to cryogenic temperatures, preserving structural heterogeneity present in solution.^{50–55} Thus, in principle, the full conformational ensemble is represented in the frozen parti-

cles, making it possible to get information about structural dynamics from cryo-EM data. However, while this is true in principle, reality is more complex as there are multiple factors that may bias the ensemble that is present in the cryo-EM grid. These include the time that it takes for the sample to freeze relative to the timescale of the structural dynamics and potential interactions between the sample, the grid substrate, and/or the water–air interface.^{50,56} Fortunately, protein-free RNAs may have a lower tendency for adsorption to the water–air interface than proteins do, as RNAs solved by cryo-EM so far do not appear to adopt preferred orientations,^{43–44,46,49} which is diagnostic for adsorption. This may be because of the relatively small size of the RNAs, their overall charge, and their solubility, but it remains to be determined whether these observations are generalizable. In addition, one feature of RNA that makes it amenable to cryo-EM is its high contrast (relative to solvent ice) in cryo-EM micrographs, which may be caused by the high electrostatic potential of its backbone. This high contrast makes it relatively easier to see even small RNA molecules during particle picking.^{26,46}

When studying RNAs that populate multiple well-defined conformations (discrete conformational heterogeneity) and/or flexible conformational states (continuous conformational heterogeneity), an advantage of cryo-EM is that data are collected for individual particles and therefore co-existing conformational states can in theory be separated and solved independently. This is one of the major advances responsible for the resolution revolution, as greater conformational homogeneity typically leads to higher-resolution structures. An interesting consequence of the single-particle nature of cryo-EM is that, in principle, cryo-EM datasets contain information about structure, conformational heterogeneity, and the relative stabilities of the different conformations.^{50,54–55} The latter is contained in the number of particles in each conformational state, which inform on the relative probabilities and therefore, the Gibbs free energies, of each conformation. Thus, in theory, if one could thoroughly and unambiguously pick particles and assign each to a specific conformational state, thermodynamic information about the conformational ensemble would be available. In practice, however, there are multiple challenges that currently limit the ability to obtain quantitative thermodynamic information from cryo-EM data. First, there may be very low signal-to-noise ratio of individual particles, which means it may be difficult to assign a given particle to a conformational state; this problem is exacerbated with small RNA molecules. Also, particle picking is imperfect and thus molecules in some states may be present in the grid but due to their shape and orientation are not detected and picked, or particles in different states may appear identical from some orientations and therefore may be difficult to classify. This will lead

to under- and over-representation of some states in the data. In addition, challenges associated with selection of correct 2D and 3D class averages could again lead to certain conformational states being underrepresented or ‘missed’ in the data. Other experimental and computational limitations also apply.

Despite the limitations mentioned above, the field has recognized the opportunity to visualize structural dynamics from cryo-EM data, and several computational tools recently have been developed for this purpose, including 3D variability analysis in cryoSPARC, multi-body refinement in Relion, and the neural network-based cryoDRGN, among others.^{51–53} These tools can help in the detection of both discrete and continuous conformational heterogeneity, and in combination with well-established classification algorithms have revealed structural dynamics in proteins and protein-nucleic acid complexes. Below, we summarize an example showing how cryo-EM can give insights into the conformational dynamics of RNA-only structures and how this affects specific molecular recognition events, in this case interaction with protein.

Conformational rearrangements of a viral RNA structure upon binding to host protein

We recently investigated a ~55 kDa RNA structure at the 3′ end of the brome mosaic virus (BMV) genome that is aminoacylated by the host’s

tyrosyl-tRNA synthetase (TyrRS) enzyme and performs multiple functions in the viral life cycle.⁴⁶ Based on its ability to be aminoacylated, the viral RNA was expected to prefold into a tRNA-like structure (TLS), but its experimentally determined secondary structure greatly differed from that of tRNA (Figure 2(A)). Despite evidence that this RNA was stably folded, it precluded crystallization for decades and it remained a mystery how the BMV TLS structure mimics tRNA.⁵⁷ Using cryo-EM, we obtained a 4.3 Å resolution map that revealed the topology of the viral RNA and allowed us to build a 3D model of the TLS and identify the location of the anticodon and acceptor arms (Figure 2(B)). Surprisingly, although the relative positions of the acceptor and anticodon arms roughly resemble those of tRNA, the 3D structure of the free TLS RNA does not fit the tRNA binding sites on the TyrRS homodimer and therefore is inconsistent with aminoacylation.⁴⁶ This suggested that the free RNA is not structurally preorganized to be recognized by TyrRS and that conformational dynamics might play a role.

Further analysis of the cryo-EM data revealed a region of the map with lower resolution, suggesting local flexibility within the structure (Figure 2(C)). To get more insights, we made use of the 3D Variability Analysis (3DVA) module within the cryoSPARC program.⁵³ This analysis uses a type of principal component analysis applied to the aligned particles to generate a set of 3D volumes that show the conformational variability con-

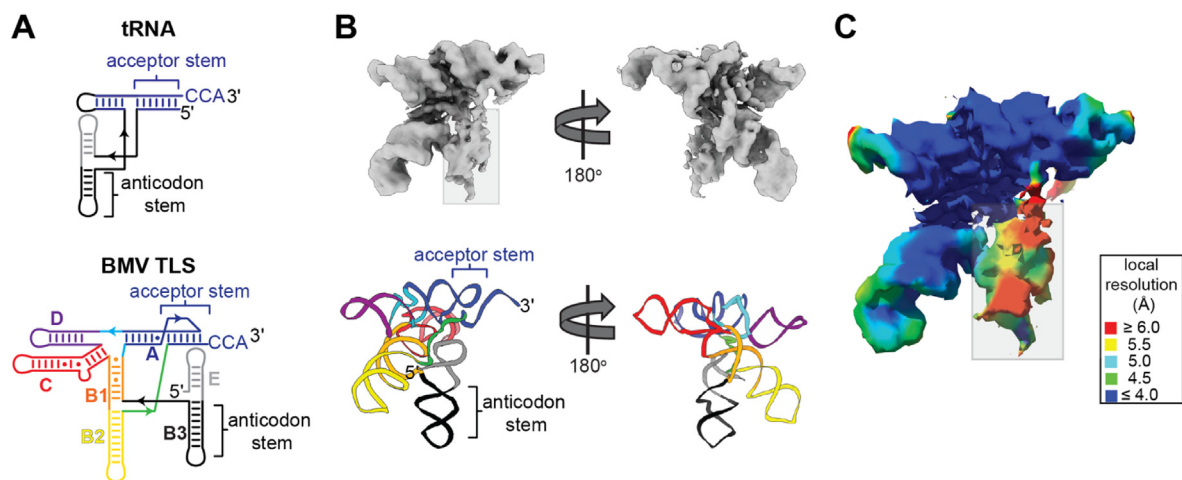
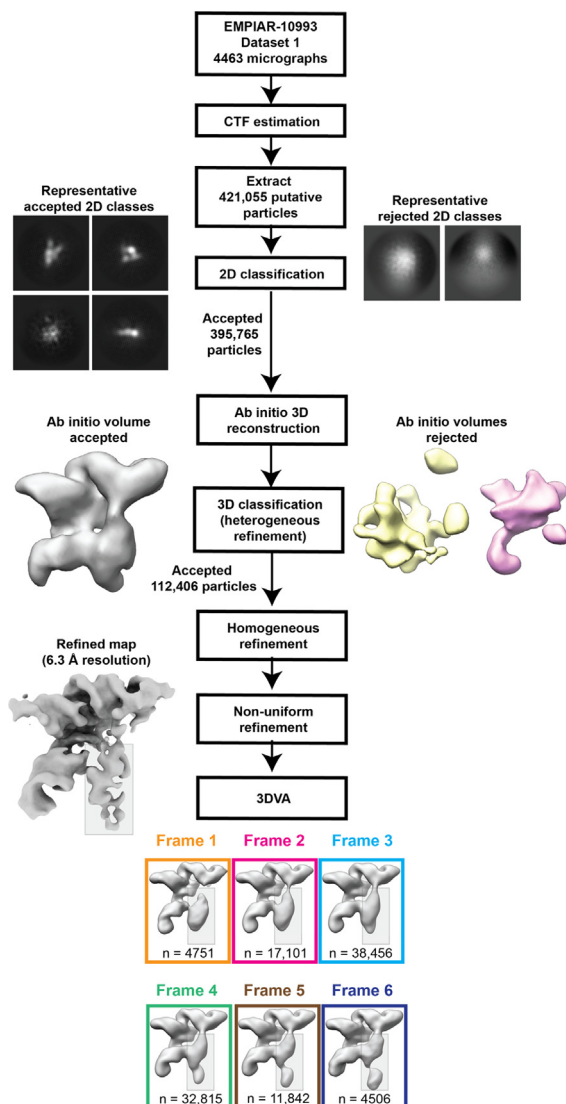


Figure 2. Cryo-EM map of viral tRNA-like structure reveals local flexibility of anticodon domain. (A) Schematic of the secondary structures of tRNA (top) and the brome mosaic virus tRNA-like structure (BMV TLS). Helices in BMV TLS are labeled (A, B1, B2, B3, C, D, and E) following naming in the literature (59). **(B)** Cryo-EM map (EMD-24952, top) and structure (PDB 7SAM, below) of the free BMV TLS RNA. The overall resolution of the map is 4.3 Å and was refined with 128,266 particles. Resolutions were calculated using a gold standard Fourier Shell Correlation (FSC) of 0.143. Grey box indicates region of the map that displayed lower resolution relative to the rest of the map. Helices in the structure are colored as in (A). **(C)** Cryo-EM map of free BMV-TLS RNA (EMD-24952) colored according to local resolution. Grey box indicates low-resolution region as in (B), suggesting it is conformationally dynamic. From S. L. Bonilla, et al., A viral RNA hijacks host machinery using dynamic conformational changes of a tRNA-like structure. *Science* **374**, 955–960 (2021). Reprinted with permission of AAAS.

tained in the dataset. To illustrate how this analysis can inform on RNA conformational dynamics, we repeat it here using a subset of the BMV TLS data deposited in the Electron Microscopy Public Image Archive (EMPIAR; Figure 3). As the goal in this case was to explore conformational variability within the dataset instead of obtaining the highest resolution possible, we performed only a limited number of 2D and 3D classifications. This served to remove junk (e.g., ice, unfolded particles, aggregates), but minimized removal of legitimate folded BMV TLS single particles. When seeking the highest resolution possible, particle classification is much more extensive to obtain the most conformationally homogenous subset possible, which can result in the disposal of some legitimate particles. In practice, it can be difficult to unambiguously distinguish junk from particles, especially when the particles are small, so it is recommended to repeat the classifications using different parameters (e.g., number of classes) to verify that the results are robust. A



6.3 Å resolution map was produced after refinement with 112,406 particles and this map was used as input for the 3DVA analysis (Figure 3). The volumes generated from this analysis can be visualized as a movie to observe putative molecular motions.

In the case of the BMV TLS, the greatest variability was localized to the anticodon arm (Figure 3), and this suggested that TyrRS recognition could involve conformational rearrangements of this domain, a testable hypothesis. This qualitative result was robust and did not change when the 3DVA parameters and/or the number of input particles changed.⁴⁶ Thus, even in the absence of a high-resolution map and without direct visualization of the conformational changes, cryo-EM provided strong initial evidence for local conformational dynamics with potential functional implications. This observation also provided a plausible explanation for the many years of futile crystallization attempts: flexibility in the RNA prevented the formation of high-quality crystals. One limitation of this analysis on the BMV TLS dataset is that the nature of the conformational changes undergone by the anticodon arm is not observable because of the overall low resolution of the map and the anticodon arm is too small for local refinements in cryoSPARC or multi-body refinement in RELION.

To test the hypothesis that the anticodon arm of the viral TLS undergoes conformational rearrangement for TyrRS recognition, we used cryo-EM to solve the structure of the TLS-TyrRS complex (Figure 4(A)).⁴⁶ Supporting the proposed hypothesis, the position of the anticodon arm in

Figure 3. Variability analysis of cryo-EM data suggests programmed structural dynamics important for binding to a host protein. (A) Diagram summarizing data processing and 3D variability analysis (3DVA) performed in cryoSPARC showing heterogeneity localized to the anticodon arm of the TLS. Analysis was performed using a subset of 4,463 motion-corrected micrographs available in public repository (dataset 1, EMPIAR-10993). Results qualitatively reproduced analysis of full dataset in original publication (46). 3DVA was performed with a map refined to 6.3 Å with 112,406 particles. Three variability components were generated (components 0, 1, and 2). Multiple “frames” along the first principal component (component 0) are shown with the number of particles used to generate each “frame” written under the volumes. Note that not all of the 112,406 particles are represented in the frames. The other two variability components (components 1 and 2; not shown) displayed relatively minor movements of other domains in BMV TLS and to a greater extent movement of domain C (Figure 2(A)). All three variability components suggest relative flexibility of the anticodon arm. For a more detailed description of the analysis on the BMV TLS dataset see ref. (46) and for a general description of cryoSPARC’s variability analysis see ref. (53).

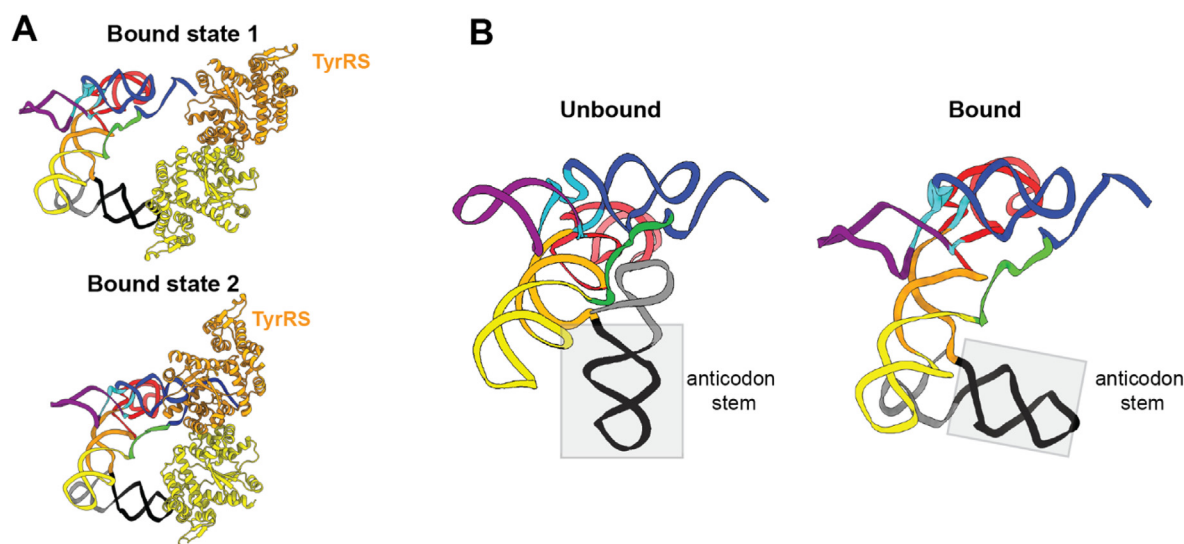


Figure 4. Cryo-EM structure of viral RNA bound to host protein confirms local conformational changes of flexible anticodon arm (A) Structures of the BMV TLS RNA bound to tyrosyl-tRNA synthetase (TyrRS) from *Phaseolus vulgaris* in two different bound states (PDB 7SC6 and 7SCQ) solved by cryo-EM. **(B)** BMV TLS RNA in bound and unbound conformations. Grey box indicates helices that undergo largest conformational rearrangements upon binding to TyrRS.

the bound viral RNA is very different to its position in the unbound state (Figure 4(B)), consistent with large conformational rearrangements upon TyrRS recognition. This contrasts with tRNA binding, as tRNA appears to be structurally preorganized for TyrRS recognition with the anticodon and acceptor arms stably connected by 3° contacts to form the canonical L-shape in the unbound state.⁵⁸ In contrast, the anticodon arm of the TLS is loosely connected to the rest of the structure by a single strand and is relatively dynamic, as revealed by the lower local resolution of this region and the variability analysis (Figure 3).

Surprisingly, the structure of the complex also revealed that the TLS binds TyrRS with a geometry that greatly differs from tRNA, with its acceptor and anticodon arms in a near parallel orientation (Figure 4(B)) rather than forming the classic L-shape of tRNA. Further, 3D classification of the particles revealed two distinct bound states (Figure 4(A)), suggesting that the TLS-TyrRS complex is also conformationally dynamic.

Put together, this example shows how cryo-EM can be applied to RNA structures in free and protein-bound forms to simultaneously solve structures, detect inherent conformational dynamics, and characterize the extent and magnitude of these dynamics. It is difficult to imagine this being possible with any other readily available structural biology technique. Conformational dynamics in both the free RNA and the RNA-protein complex were detected and thus preliminary insight into these ensembles was obtained with no prior knowledge that these dynamics existed. These analyses, while not

rigorously quantitative, give insights into the molecule's conformational ensemble. Once this information is available, new hypotheses that include structural dynamics can be generated, and new experiments can be designed to test these dynamics-based mechanistic models.

Conclusions

Although much of the attention of the last few years has been focused on the ability of cryo-EM to produce high-resolution structures, the so-called “resolution revolution”, some of the most exciting developments will be in the use of cryo-EM to get insights into structural dynamics in a way not previously possible. The ability to separate distinct conformations within a sample is one of the greatest advantages of cryo-EM over other tools and in the next few years we imagine more and more complex motions being analyzed by increasingly sensitive and sophisticated software tools. As we described above, RNA structures are more conformationally dynamic than proteins and therefore RNA structural biology will greatly benefit from these advances in cryo-EM. As illustrated by the BMV TLS-TyrRS complex, RNAs often work in concert with proteins and advances in cryo-EM that enhance our understanding of RNA structure and conformational dynamics will also benefit our understanding of the mechanism by which RNA-protein complexes form and function. Also, carefully considering how sample preparation, data collection, and data analyses could be made

more quantitative could yield great dividends by potentially allowing measurement of the relative populations in each of the observed conformational states. Cryo-EM has already shown great potential for solving the structures of small conformationally dynamic RNAs in their free and protein-bound forms. In the next few years, we expect an explosion in the number of RNA structures solved by cryo-EM and in our understanding of RNA structural dynamics and their relation to biological function. In many ways, the revolution is just beginning.

CRedit authorship contribution statement

Steve L. Bonilla: Conceptualization, Investigation, Formal analysis, Writing – original draft, Writing – review & editing, Funding acquisition. **Jeffrey S. Kieft:** Conceptualization, Writing – original draft, Writing – review & editing, Supervision, Project administration, Funding acquisition.

DECLARATION OF COMPETING INTEREST

The authors declare that they have no known competing financial interests or personal relationships that could have appeared to influence the work reported in this paper.

Acknowledgements

The authors wish to thank current members of the Kieft Lab for helpful discussions. Theo Humphreys (PNCC) and Eduardo Romero (UC Anschutz) assisted with microscope operation. Dave Farrell provided support of computational resources. This work was funded by National Institutes of Health grant R35GM118070 to J. S.K. and by a HHMI Hanna H. Gray fellowship awarded to S.L.B. A portion of this research was supported by NIH grant U24GM129547 and performed at the PNCC at OHSU and accessed through EMSL (grid.436923.9), a DOE Office of Science User Facility sponsored by the Office of Biological and Environmental Research.

Received 12 May 2022;
Accepted 24 August 2022;
Available online 29 August 2022

Keywords:

Cryo-electron microscopy;
RNA structure;
RNA conformational dynamics;
RNA cryo-EM;
RNA folding;
RNA thermodynamics

References

- Herschlag, D., Bonilla, S., Bisaria, N., (2018). The Story of RNA Folding, as Told in Epochs. *Cold Spring Harb Perspect. Biol.* **10**
- Vicens, Q., Kieft, J.S., (2022). Thoughts on how to think (and talk) about RNA structure. *Proc. Natl. Acad. Sci. U S A* **119** e2112677119.
- Cech, T.R., Steitz, J.A., (2014). The noncoding RNA revolution-trashing old rules to forge new ones. *Cell* **157**, 77–94.
- Ganser, L.R., Kelly, M.L., Herschlag, D., Al-Hashimi, H.M., (2019). The roles of structural dynamics in the cellular functions of RNAs. *Nat. Rev. Mol. Cell Biol.* **20**, 474–489.
- Bonomi, M., Heller, G.T., Camilloni, C., Vendruscolo, M., (2017). Principles of protein structural ensemble determination. *Curr. Opin. Struct. Biol.* **42**, 106–116.
- Ke, A., Doudna, J.A., (2004). Crystallization of RNA and RNA-protein complexes. *Methods* **34**, 408–414.
- Leontis, N.B., Lescoute, A., Westhof, E., (2006). The building blocks and motifs of RNA architecture. *Curr. Opin. Struct. Biol.* **16**, 279–287.
- Lescoute, A., Leontis, N.B., Massire, C., Westhof, E., (2005). Recurrent structural RNA motifs, Isostericity Matrices and sequence alignments. *Nucleic Acids Res.* **33**, 2395–2409.
- Bonilla, S.L. et al, (2021). High-throughput dissection of the thermodynamic and conformational properties of a ubiquitous class of RNA tertiary contact motifs. *Proc. Natl. Acad. Sci. U S A* **118**
- Denny, S.K. et al, (2018). High-Throughput Investigation of Diverse Junction Elements in RNA Tertiary Folding. *Cell* **174**, 377–390 e320.
- Yesselman, J.D. et al, (2019). Sequence-dependent RNA helix conformational preferences predictably impact tertiary structure formation. *Proc. Natl. Acad. Sci. U S A* **116**, 16847–16855.
- Stelzer, A.C. et al, (2011). Discovery of selective bioactive small molecules by targeting an RNA dynamic ensemble. *Nat. Chem. Biol.* **7**, 553–559.
- Haller, A., Souliere, M.F., Micura, R., (2011). The dynamic nature of RNA as key to understanding riboswitch mechanisms. *Acc. Chem. Res.* **44**, 1339–1348.
- Serganov, A., Patel, D.J., (2012). Molecular recognition and function of riboswitches. *Curr. Opin. Struct. Biol.* **22**, 279–286.
- Haller, A., Rieder, U., Aigner, M., Blanchard, S.C., Micura, R., (2011). Conformational capture of the SAM-II riboswitch. *Nat. Chem. Biol.* **7**, 393–400.
- Rodgers, M.L., Woodson, S.A., (2021). A roadmap for rRNA folding and assembly during transcription. *Trends Biochem. Sci.* **46**, 889–901.
- Gianni, S., Dogan, J., Jemth, P., (2014). Distinguishing induced fit from conformational selection. *Biophys. Chem.* **189**, 33–39.
- Rinn, J.L., Chang, H.Y., (2012). Genome regulation by long noncoding RNAs. *Annu. Rev. Biochem.* **81**, 145–166.
- Zampetaki, A., Albrecht, A., Steinhofel, K., (2018). Long Non-coding RNA Structure and Function: Is There a Link? *Front. Physiol.* **9**, 1201.
- Sponer, J. et al, (2018). RNA Structural Dynamics As Captured by Molecular Simulations: A Comprehensive Overview. *Chem. Rev.* **118**, 4177–4338.

21. Salmon, L., Yang, S., Al-Hashimi, H.M., (2014). Advances in the determination of nucleic acid conformational ensembles. *Annu. Rev. Phys. Chem.* **65**, 293–316.
22. Shi, H. et al, (2020). Rapid and accurate determination of atomistic RNA dynamic ensemble models using NMR and structure prediction. *Nat. Commun.* **11**, 5531.
23. Zhang, X.J., Wozniak, J.A., Matthews, B.W., (1995). Protein flexibility and adaptability seen in 25 crystal forms of T4 lysozyme. *J. Mol. Biol.* **250**, 527–552.
24. Burra, P.V., Zhang, Y., Godzik, A., Stec, B., (2009). Global distribution of conformational states derived from redundant models in the PDB points to non-uniqueness of the protein structure. *Proc. Natl. Acad. Sci. U S A* **106**, 10505–10510.
25. Vekilov, P.G., Chung, S., Olafson, K.N., (2016). Shape change in crystallization of biological macromolecules. *MRS Bull.* **41**, 375–380.
26. Ma, H., Jia, X., Zhang, K., Su, Z., (2022). Cryo-EM advances in RNA structure determination. *Signal Transduct. Target Ther.* **7**, 58.
27. Scott, L.G., Hennig, M., (2008). RNA structure determination by NMR. *Methods Mol. Biol.* **452**, 29–61.
28. Zhang, H., Keane, S.C., (2019). Advances that facilitate the study of large RNA structure and dynamics by nuclear magnetic resonance spectroscopy. *Wiley Interdiscip. Rev. RNA* **10**, e1541.
29. Walter, N.G., (2003). Probing RNA structural dynamics and function by fluorescence resonance energy transfer (FRET). *Curr. Protoc. Nucleic Acid Chem.* **Chapter 11**, 111011–111023.
30. Shi, X., Bonilla, S., Herschlag, D., Harbury, P., (2015). Quantifying Nucleic Acid Ensembles with X-ray Scattering Interferometry. *Methods Enzymol.* **558**, 75–97.
31. Tomezsko, P.J. et al, (2020). Determination of RNA structural diversity and its role in HIV-1 RNA splicing. *Nature* **582**, 438–442.
32. Spasic, A., Assmann, S.M., Bevilacqua, P.C., Mathews, D. H., (2018). Modeling RNA secondary structure folding ensembles using SHAPE mapping data. *Nucleic Acids Res.* **46**, 314–323.
33. Bonilla, S. et al, (2017). Single-Molecule Fluorescence Reveals Commonalities and Distinctions among Natural and in Vitro-Selected RNA Tertiary Motifs in a Multistep Folding Pathway. *J. Am. Chem. Soc.* **139**, 18576–18589.
34. Plumridge, A. et al, (2018). Revealing the distinct folding phases of an RNA three-helix junction. *Nucleic Acids Res.* **46**, 7354–7365.
35. Pollack, L., (2011). Time resolved SAXS and RNA folding. *Biopolymers* **95**, 543–549.
36. Pollack, L., Doniach, S., (2009). Time-resolved X-ray scattering and RNA folding. *Methods Enzymol.* **469**, 253–268.
37. Bernetti, M., Hall, K.B., Bussi, G., (2021). Reweighting of molecular simulations with explicit-solvent SAXS restraints elucidates ion-dependent RNA ensembles. *Nucleic Acids Res.* **49**, e84.
38. Mathew-Fenn, R.S., Das, R., Silverman, J.A., Walker, P.A., Harbury, P.A., (2008). A molecular ruler for measuring quantitative distance distributions. *PLoS ONE* **3**, e3229.
39. Kuhlbrandt, W., (2014). Cryo-EM enters a new era. *Elife* **3**, e03678.
40. Bai, X.C., McMullan, G., Scheres, S.H., (2015). How cryo-EM is revolutionizing structural biology. *Trends Biochem. Sci.* **40**, 49–57.
41. Kuhlbrandt, W., (2014). Biochemistry. The resolution revolution. *Science* **343**, 1443–1444.
42. Wu, M., Lander, G.C., (2020). How low can we go? Structure determination of small biological complexes using single-particle cryo-EM. *Curr. Opin. Struct. Biol.* **64**, 9–16.
43. Zhang, K., Li, S., Kappel, K., Pintilie, G., Su, Z., Mou, T.C., Schmid, M.F., Das, R., et al., (2019). Cryo-EM structure of a 40 kDa SAM-IV riboswitch RNA at 3.7 Å resolution. *Nat. Commun.* **10**
44. Su, Z. et al, (2021). Cryo-EM structures of full-length Tetrahymena ribozyme at 3.1 Å resolution. *Nature* **596**, 603–607.
45. Liu, D., Thelot, F.A., Piccirilli, J.A., Liao, M., Yin, P., (2022). Sub-3-Å cryo-EM structure of RNA enabled by engineered homomeric self-assembly. *Nat. Methods.*
46. Bonilla, S.L., Sherlock, M.E., MacFadden, A., Kieft, J.S., (2021). A viral RNA hijacks host machinery using dynamic conformational changes of a tRNA-like structure. *Science* **374**, 955–960.
47. Zhang, K. et al, (2021). Cryo-EM and antisense targeting of the 28-kDa frameshift stimulation element from the SARS-CoV-2 RNA genome. *Nat. Struct. Mol. Biol.* **28**, 747–754.
48. Bonilla, S.L., Vicens, Q., Kieft, J.S., (2022). Cryo-EM reveals an entangled kinetic trap in the folding pathway of a catalytic RNA. *Sci. Adv.* **8** (34) <https://doi.org/10.1126/sciadv.abq4144>.
49. Kappel, K. et al, (2020). Accelerated cryo-EM-guided determination of three-dimensional RNA-only structures. *Nat. Methods* **17**, 699–707.
50. Bock, L.V., Grubmuller, H., (2022). Effects of cryo-EM cooling on structural ensembles. *Nat. Commun.* **13**, 1709.
51. Zhong, E.D., Bepler, T., Berger, B., Davis, J.H., (2021). CryoDRGN: reconstruction of heterogeneous cryo-EM structures using neural networks. *Nat. Methods* **18**, 176–185.
52. Nakane, T., Kimanius, D., Lindahl, E., Scheres, S.H., (2018). Characterisation of molecular motions in cryo-EM single-particle data by multi-body refinement in RELION. *Elife* **7**
53. Punjani, A., Fleet, D.J., (2021). 3D variability analysis: Resolving continuous flexibility and discrete heterogeneity from single particle cryo-EM. *J. Struct. Biol.* **213**, 107702.
54. Giraldo-Barreto, J. et al, (2021). A Bayesian approach to extracting free-energy profiles from cryo-electron microscopy experiments. *Sci. Rep.* **11**, 13657.
55. Bonomi, M., Pellarin, R., Vendruscolo, M., (2018). Simultaneous Determination of Protein Structure and Dynamics Using Cryo-Electron Microscopy. *Biophys. J.* **114**, 1604–1613.
56. Noble, A.J. et al, (2018). Reducing effects of particle adsorption to the air-water interface in cryo-EM. *Nat. Methods* **15**, 793–795.
57. Hammond, J.A., Rambo, R.P., Filbin, M.E., Kieft, J.S., (2009). Comparison and functional implications of the 3D architectures of viral tRNA-like structures. *RNA* **15**, 294–307.
58. Tsunoda, M. et al, (2007). Structural basis for recognition of cognate tRNA by tyrosyl-tRNA synthetase from three kingdoms. *Nucleic Acids Res.* **35**, 4289–4300.